

# Ignition Transient of Supercritical Oxygen/Kerosene Combustion System

Dohun Kim, Keunwoong Lee  
Graduate School of Korea Aerospace University  
Goyang, Gyeonggi, Republic of Korea

Jaye Koo  
Korea Aerospace University  
Goyang, Gyeonggi, Republic of Korea

## 1 Introduction

The propellants of large liquid rocket engine are mixed and burned in supercritical pressure and temperature condition. Generally, the critical temperature and pressure of liquid rocket engine propellants are much lower than the propellant feed, injection and combustion condition [1-3]. In the super-critical condition, the distinction between liquid and gas phase would be obscure, and the thermodynamic and fluid-dynamic properties of both a liquid phase (high density) and a gas phase (low viscosity, zero surface tension, and high thermal diffusivity) coexist [4-6]. Before ignition, the propellants are injected under subcritical condition. At the moment of ignition, the pressure and temperature increase drastically, there would be a transition of thermodynamic state from subcritical to supercritical state. Many researchers studied the ignition and high pressure combustion of liquid rocket engine by visualizing the combustion flow field and the free radical distribution[7-10]. However, most of their studies focused on the sub to supercritical combustion of cryogenic fuel such as hydrogen and methane, and there are not enough experimental studies about the ignition phenomenon of kerosene fuel using optical method.

In this study, the ignition transient of a gaseous oxygen/kerosene spray was visualized using a windowed subscale liquid rocket combustor, which is operated at a supercritical combustion pressure.

## 2 Experimental Setup

The shear coaxial injector was designed for high pressure combustion experiment. The injector assembly consists of two parts – center post and outer body – as shown in Fig. 1 (a). The pressure drops at gas and liquid injectors were determined using metering orifices, which are inserted in the propellant inlet ports of injector. The geometrical dimensions and the operating conditions are listed in Table 1. In order to observe the high pressure combustion flow field of GOx/kerosene spray, the windowed combustor was designed as shown in Fig. 1 (b). The inner diameter and the overall length from the injector face plate to the nozzle throat are 22 mm and 182 mm respectively. The combustor

body consists of three modules; (i)upstream module for flame visualization and igniter attachment, (ii)middle module for adjusting combustor length, and (iii)downstream module with exhaust nozzle and water cooling channel. The propellants spray was ignited using a motorcycle spark plug(NGK CR8EIX) and a high voltage induction coil(11kV).

The spray flowfield at the ignition transient was observed using shadowgraph visualization technique. Since the luminosity of kerosene flame is very high due to the black body emission of carbon particle, the higher intensity of light source was required to exclude the light emission of flame from the shadowgraph image. The light source we used is a 27 Watts high power light emitting diode, which has a claimed 2100 lumens. The light is collimated to a parallel light using a plano-convex lens with a focal length of 300mm. The parallel light passes by the combustion flowfield through two quartz windows, and is focused on the CCD arrays of Photron APX-RS high speed camera. The ignition sequence is controlled by a custom-made MCU-based controller, and the time-chart is represented in Fig. 4. Although the oxidizer valve opening signal is transmitted 500 ms faster than the fuel valve opening signal, the oxidizer and fuel are injected almost simultaneously due to the difference of filling time for the volume between the valve and the injector.

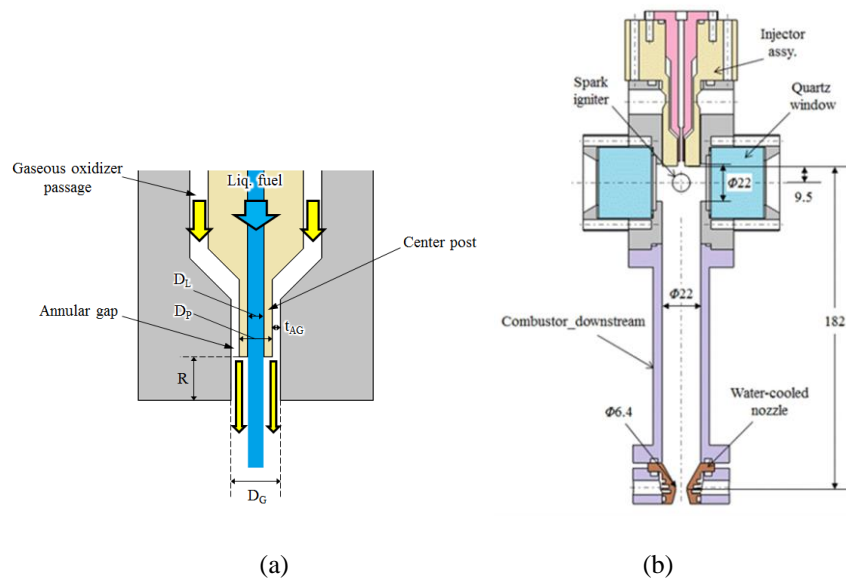


Figure 1. Schematic of (a) shear coaxial type injector and (b) subscale windowed combustor

Table 1. Geometrical dimensions of GOx/Kerosene coaxial injector and combustor.

Geometrical dimensions of injector	
Liquid center post I.D., $D_L$	1.5 mm
Liquid center post O.D., $D_P$	3.0 mm
Annular gap width, $t_{AG}$	0.75 mm
Outer body I.D., $D_G$	4.5 mm
Recess depth, $R$	3.0 mm
Geometrical dimensions of combustor	
Length from injector to nozzle throat	182 mm
Inner diameter	22 mm
Nozzle throat diameter	6.4 mm

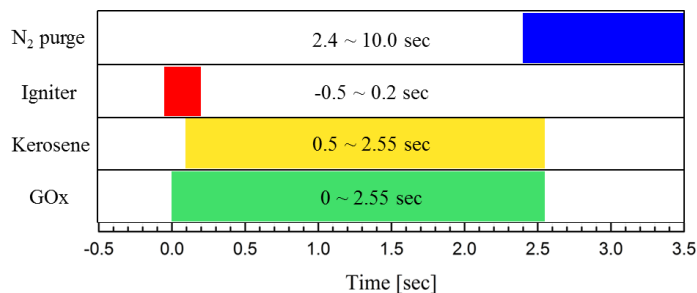


Figure 4. Time-table of hot-firing sequence

### 3 Results and Discussion

The hot-firing experiment was carried out using subscale windowed combustor and GOx/kerosene propellants. The flow and combustion conditions are listed in Table 2. The combustion pressure at steady state was 28.1 bar, and it is 12% higher than the critical pressure of kerosene (approx. 25bar). The total mass flow rate was 48g/s, and the oxidizer to fuel mass ratio was 2.53. Figure 3 (a) and (b) show the pressure traces during the entire combustion period and the ignition moment respectively. Since the combustion pressure transducer has an orifice at the sensing port for protecting the piezo element from pressure peak, the combustion pressure,  $P_{cc}$  increased gradually. For that reason, the real time combustion pressure could not be compared with the high speed shadowgraph images. The oxidizer injection pressure,  $P_{ox, inj.}$  was measured at the downstream of the oxidizer control valve, so  $P_{ox, inj.}$  was increased from 0 bar after oxidizer valve opening. However, since the fuel injection pressure,  $P_{f, inj.}$  was measured at the upstream of the fuel control valve,  $P_{f, inj.}$  was dropped from the fuel supply pressure, 44bar. The pressure transducers for  $P_{ox, inj.}$  and  $P_{f, inj.}$  have no damping orifice at their pressure measuring ports, so the injection pressure measurements exhibit a delay time under 1ms as the manufacturer claimed.

According to the fuel injection pressure plot in Fig. 3 (b), the ignition was occurred in 18 to 25 ms after the opening of fuel valve. The sequential shadowgraph images in Fig. 4 show that the ignition was initiated at 22ms after the beginning of propellant injection. This means that the time scales of pressure data and the high speed shadowgraph images coincide with each other approximately. Before ignition, the unburnt propellant spray showed general breakup behavior of coaxial gas-liquid spray. When the flammable mixture reached the arc-discharging region of spark plug gap, the yellow flame propagated to the entire area of visualized region within 1ms. Fig. 5 is sequential shadowgraph images at the moment of ignition. The change of background color in 22.2 and 29.3ms of Fig. 4 and bottom row images of Fig. 5 are caused by the yellow flame of high luminosity. As shown in Fig. 4 and 5, the spray core was disappeared for about 25 ms. Although the exact combustion pressure could not be verified at that moment, it can be deduced that there was reversal pressure gradient at the injector, which was due to simultaneous release of a large amount of energy from unburnt propellant that was accumulated in the combustion chamber. The propellant spray injection discontinued immediately after the ignition, and the injected spray began to be consumed by vaporization and combustion reaction as shown in 22.2-22.5ms images of Fig. 5. 25ms later from the ignition, the spray was re-injected with high fluctuation of liquid jet and combustion reaction. The yellow flame was observed only at the downstream of spray, where the dense spray disappeared completely within about 10mm from the injector face plate as shown in 47.7-50.2ms of Fig. 4. This phenomenon was caused by rapid diffusion of kerosene jet under supercritical condition. Though the temperature of propellant spray was not measured, we could infer that the temperature of kerosene spray increased rapidly over critical

temperature of kerosene (676K) by convective and radiative heat transfer from combustion gas recirculation [11] and black body radiation [12] respectively. The reactive spray was stabilized 40 ms later from the ignition. The stabilization of spray was determined from spray core length detection result in Fig. 6. The stabilization point of reactive spray was defined as the time when the spray core length was in  $\pm 20\%$  of steady state average after overshoot.

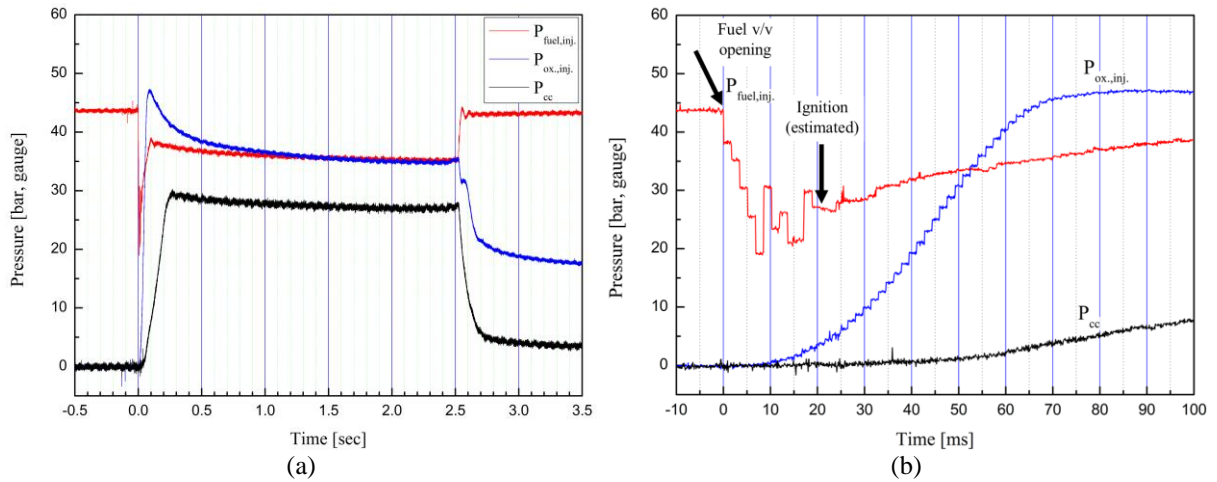


Figure 3. Pressure traces measured during (a)entire hot-firing and (b)ignition process.

0 ms	5.3 ms	19.8 ms	22.2 ms	29.3 ms
Initiation of GOx/Kerosene spray	Developing spray	Shear interaction and mixing of unburnt spray	Ignition, flame propagation	Rapid increase of combustion pressure
46.2 ms	47.7 ms	50.2 ms	62.2 ms	1000 ms
Initiation of propellant re-injection	Re-developing of propellant spray	Stabilization of reactive GOx/Kerosene spray	Stabilized reactive spray	Steady state

Figure 4. Behaviors of GOx/kerosene spray during hot-firing, time: elapsed time after fuel valve opening.

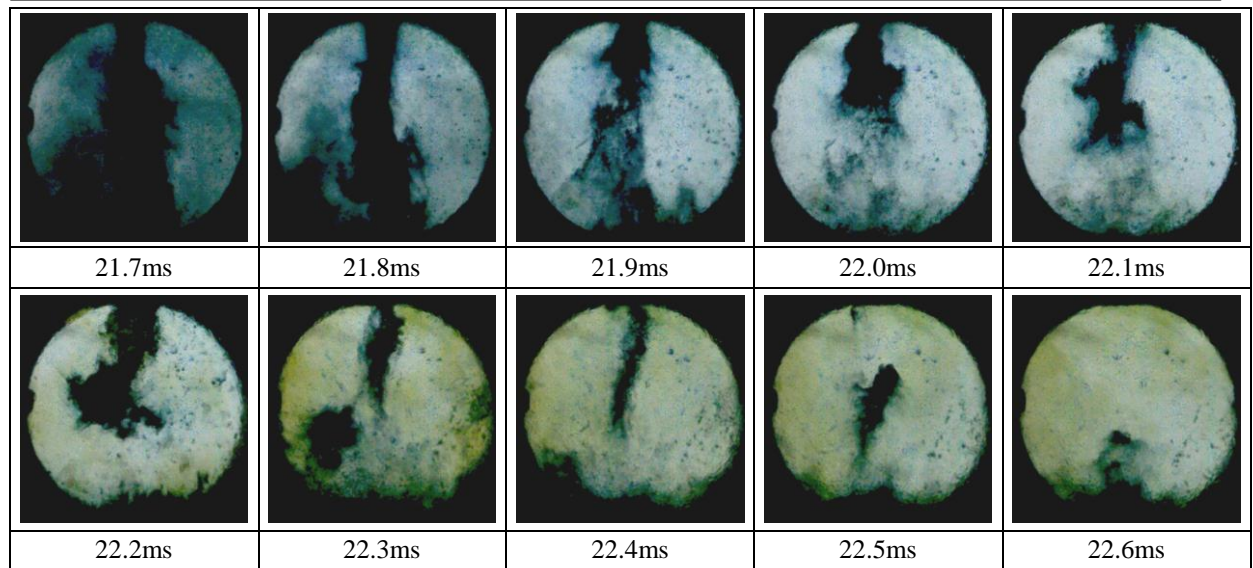


Figure 5. Spray behavior at moment of ignition, time: elapsed time after fuel valve opening.

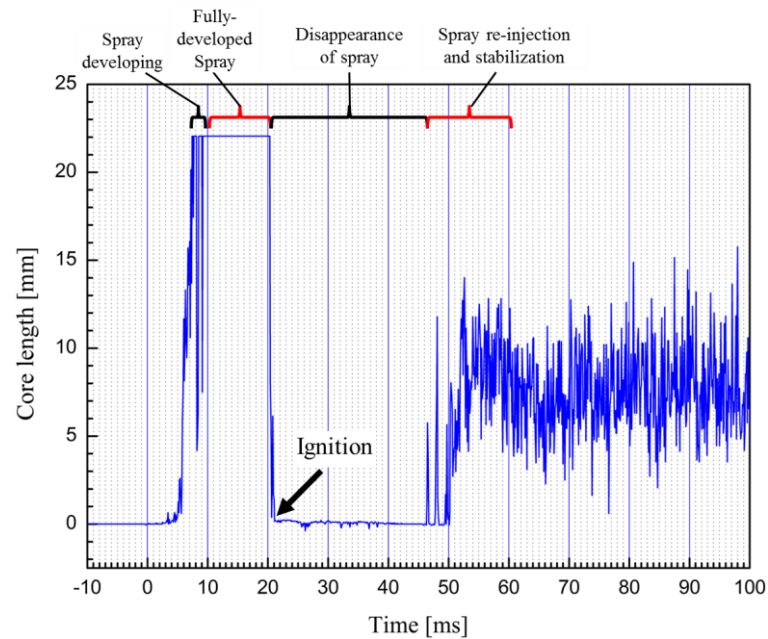


Figure 6. Time-change of estimated spray core length at ignition transient

## 4 Conclusion

The ignition transient of gaseous oxygen/kerosene spray was successfully observed with the windowed combustor and the shadowgraph apparatus. The intense light emission from kerosene flame was excluded from shadowgraph image using the improved light source. In order to understand the ignition process more clearly, the pressure history, the high speed shadowgraph images, and the time trace of estimated spray core length were compared each other. The peak pressure at ignition moment

caused the instantaneous discontinuance of propellant injection. The re-injected GOx/kerosene spray showed rapid mixing and combustion, which was induced by the change of thermodynamic state of kerosene from sub- to supercritical condition.

## References

- [1] Manski D, et al. (1998). Cycles for Earth-to-Orbit Propulsion. *J. Propuls. Power.* 14: 588.
- [2] Sutton GP. (2003). History of Liquid Propellant Rocket Engines in the United States. *J. Propuls. Power.* 19: 978.
- [3] Sutton GP. (2003). History of Liquid-Propellant Rocket Engines in Russia, Formerly the Soviet Union. *J. Propuls. Power.* 19: 1008.
- [4] Cengel YA, Boles MA. (2005). *Thermodynamics: An Engineering Approach*. 5th ed. McGraw-Hill College (ISBN 0-07-288495-9).
- [5] Smith JJ et al. (2004) High Pressure LOx/H<sub>2</sub> Combustion & Flame Dynamics Preliminary Results. *Proc. 40th AIAA/ASME/SAE/ASEE Jt. Propuls. Conf. Exhib.:* AIAA 2004-3376.
- [6] Zhong F et al. (2012). Characteristics of compressible flow of supercritical kerosene. *Acta Mech. Sin.* 28: 8.
- [7] Mayer W et al. (2004). Propellant atomization and ignition phenomena in liquid oxygen/gaseous hydrogen rocket combustors. *J. Propuls. Power.* 17: 794.
- [8] Mayer W et al. (1998) Atomization and Breakup of Cryogenic Propellants Under High-Pressure Subcritical and Supercritical Conditions. *J. Propuls. Power.* 14: 835.
- [9] Lux J, Haidn O. (2009). Flame stabilization in high-pressure liquid oxygen/methane rocket engine combustion. *J. Propuls. Power.* 25: 15.
- [10] Locke J et al. (2010). High speed visualization of LOx/GH<sub>2</sub> rocket injector flow field: hot-fire and cold-flow experiments. *Proc. 46th AIAA/ASME/SAE/ASEE Jt. Propuls. Conf. Exhib.:* AIAA 2010-7145.
- [11] Singla G et al. (2006) Planar laser-induced fluorescence of OH in high-pressure cryogenic LOx/GH<sub>2</sub> jet flames. *J. Comb. Flame.* 144: 151.
- [12] Linck M, Gupta AK. (2003) Effect of Swirl and Combustion on Flow Dynamics in Luminous Kerosene. *Proc. 41st Aerospace Sciences Meeting and Exhib.:* AIAA 2003-1345.